Oral presentation | Numerical methods

Numerical methods-VI

Thu. Jul 18, 2024 10:45 AM - 12:45 PM Room A

[10-A-03] A new subgrid-scale model for large eddy simulations of incompressible turbulent flows within the lattice Boltzmann framework

*Heng Zhang[1], Haibao Hu （1. NorthWestern Polytechnical University）

Keywords: Lattice Boltzmann method, turbulence, large eddy simulations

Twelfth International Conference on Computational Fluid Dynamics (ICCFD12), Kobe, Japan, July 14-19, 2024

A new subgrid-scale model for large eddy simulations of incompressible turbulent flows within the lattice Boltzmann framework

Heng Zhang*, Haibao Hu*
Corresponding author: huhaibao@nwpu.edu.cn
* School of Marine Science and Technology, Northwestern Polytechnical University, Xi'an, Shaanxi 710072, People's Republic of China

Abstract: Turbulent flow is an important and difficult problem in fluid mechanics because of its high-dimensional, random, multi-scale, and nonlinear characteristics[1]. Among many numerical research methods, large eddy simulations (LES) are a popular method for turbulent simulations because of their accuracy and efficiency. Here, A new coupling model is proposed that combines non-equilibrium moments and the subgrid-scale model was proposed within the framework of the lattice Boltzmann method (LBM)[2]. The new model establishes a relation between the non-equilibrium moments and the eddy viscosity by using a special calculation form of the subgrid-scale model and Chapman-Enskog analysis. The coupling model is validated in three typical three-dimensional (3D) flow cases: freely decaying homogeneous isotropic turbulence, homogeneous isotropic turbulence with body forces[3] and incompressible turbulent channel flow at Re_τ=180 according to the half height of the channel. Under the 3D Cartesian coordinate system, D3Q19 discretization scheme is applied in the core numerical solver for momentum evolution in the LBM. The results show that the new model is accurate and efficient when compared with the results of direct numerical simulations (DNS). While in the turbulent channel flow, the new model has lower numerical dissipation close to the wall. Using calculation format of the eddy viscosity, a uniform calculation format is used for each grid point of the flow field during the modeling process. The modeling process uses only the local distribution function to obtain the local eddy viscosity without any additional processing on the boundary, while optimizing the memory access process to fit the inherent parallelism of the LBM. The efficiency of computation is improved by about 20% compared to the central difference method (CDM) approach for obtaining the eddy viscosity.

Keywords: Lattice Boltzmann method, large eddy simulations, incompressible turbulent flows.

1 Introduction

The numerical simulation of turbulence is an important and difficult problem in computational fluid mechanics. At present, there are three numerical simulation methods for turbulent flow, namely direct numerical simulations (DNS), large eddy simulations (LES), and Reynolds Average Navier-Stokes (RANS), according to the different methods for solving Navier–Stokes equations. The LES uses a spatial filtering method, which divides the vortices in the flow field into large and small scale vortices [4]. The large scale vortices are directly solved, and the small scale vortices are modeled by subgrid-scale model. Compared with the other two methods, LES can take into account both the computation amount and the computation accuracy. Therefore, LES have gradually become a popular method and has been applied in numerical simulation of turbulent flow [5].

In recent years, as a rapidly developed numerical simulation method, LBM has attracted a large number of researchers. Different from the traditional finite volume method (FVM) and finite element method (FEM), LBM mainly realizes the time and space evolution process of the flow field based on the distribution function of mesoscopic scale. In the LBM, the processing of distribution function is mainly divided into two processes: collision and streaming processes [6].

In process of collision, the calculation of each point in the flow field is independent of the variables of the surrounding grid points, which is also the main reason for the good parallelism of LBM. Another obvious difference from the traditional method is that LBM can obtain the shear strain rate tensor through the non-equilibrium distribution functions (or non-equilibrium moments), rather than directly from the macroscopic velocity. In addition, LBM has many advantages such as simple boundary processing, clear physical meaning and has been widely used in computational fluid mechanics [7-10].

LES for the turbulence is also an important direction in the LBM community[11, 12]. Some common subgrid-scale models are like Smagorinsky model [13], the Vreman model [14], and the dynamic Vreman model [15], as well as the wall-adaptive local eddy (WALE) model [16], the σ model [17], volumetric strain-stretching (VSS) model [18]. Smagorinsky model is the first proposed subgrid-scale model, which has achieved satisfactory results in the homogeneous turbulent flow, but in the wall-bounded turbulent flow, Smagorinsky model is overdissipative near the wall.

It should be noted that all of the subgrid-scale models described above, except the Smagorinsky model, require a complete calculation of the velocity gradient tensor. However, the newly proposed VSS model this year only needs to calculate the shear strain rate tensor to complete the calculation of eddy viscosity. So far, the VSS model has been applied to the simulation of isotropic homogeneous turbulence and compressible/incompressible wall-bounded turbulence [18]. As far as we know, there is little research of combining non-equilibrium distribution function with VSS model.

Based on this, we propose an algorithm that combines the VSS model with the LBM non-equilibrium distribution function to achieve large eddy simulation of turbulence, and we use three typical flow problems to verify our newly proposed algorithm, they are freely decaying homogeneous isotropic turbulence, homogeneous isotropic turbulence with body forces and incompressible turbulent channel flow at $Re_\tau = 180$ according to the half height of the channel.

2 Numerical Methods

2.1 Subgrid-scale modeling

The governing equations of the incompressible LES can be written as

$$\begin{cases} \dfrac{\partial \bar{u}_i}{\partial x_i} = 0 \\ \rho_0 \left(\dfrac{\partial \bar{u}_i}{\partial t} + \dfrac{\partial \bar{u}_i \bar{u}_j}{\partial x_j} \right) = -\dfrac{\partial \bar{p}}{\partial x_i} - \rho_0 \dfrac{\partial \tau_{ij}}{\partial x_j} + \rho_0 \nu_0 \dfrac{\partial^2 \bar{u}_i}{\partial x_j x_j} + \bar{F}_i \end{cases} \tag{1}$$

where $\bar{u}_i$, $\bar{p}$, and $\bar{F}_i$ represent the resolved velocity, pressure, and force in the fluid field, respectively, ρ_0 is the density of the fluid, ν_0 represents the molecular viscosity. $\tau_{ij} = \overline{u_i u_j} - \bar{u}_i \bar{u}_j$, represents the SGS stress. Base on the eddy-viscosity assumption,

$$\tau_{ij} - \frac{1}{3}\delta_{ij}\tau_{kk} = -2\nu_t \bar{S}_{ij} \tag{2}$$

where ν_t is the eddy viscosity, and it can be obtained by the local velocity gradient tensor. $\bar{S}_{ij} = (\partial_i \bar{u}_j + \partial_j \bar{u}_i)/2$ is the strain tensor. For the ν_t, different SGS models have different algorithms, but can be represented using a general formula,

$$\nu_t = (C_{vis}\bar{\Delta})^2 f(\nabla \mathbf{u}) \tag{3}$$

where C_{vis} is a constant coefficient. $\bar{\Delta}$ is the filter scale, and $f(\nabla \mathbf{u})$ is a function of the velocity gradient tensor. The classical Smagorinksy model can be written as

$$\nu_t = (C_{vis}\bar{\Delta})^2 |\bar{S}| \tag{4}$$

where C_{vis} takes values in the range of 0.1-0.2, $|\bar{S}|$ is the mode of the $\bar{S}_{ij}$ and $|\bar{S}| = (2\bar{S}_{ij}\bar{S}_{ij})^{1/2}$.

The VSS model,

$$R_{ij} = \begin{pmatrix} S_{23}S_{11} & S_{23}S_{22} & S_{23}S_{33} \\ S_{13}S_{11} & S_{13}S_{22} & S_{13}S_{33} \\ S_{12}S_{11} & S_{12}S_{22} & S_{12}S_{33} \end{pmatrix} \tag{5}$$

$$\nu_t = (C_{vis}\overline{\Delta})^2 \frac{(\bar{R}_{ij}\bar{R}_{ij})^{\frac{3}{2}}}{(\bar{S}_{ij}\bar{S}_{ij})^{\frac{5}{2}}} \tag{6}$$

where C_{vis} is a constant and the recommended value is 1.3 [18].

2.2 Coupling algorithm of LBM and VSS model

The LBM equation based on the multiple-relaxation time model can be written as

$$\boldsymbol{f}(\mathbf{x}+\mathbf{e}_i\delta t, t+\delta t) - \boldsymbol{f}(\mathbf{x},t) = -(\mathbf{M}^{-1}\boldsymbol{\Lambda}\mathbf{M})[\boldsymbol{f}(\mathbf{x},t) - \boldsymbol{f}^{eq}(\mathbf{x},t)] + [\mathbf{M}^{-1}(\mathbf{I}-\frac{\boldsymbol{\Lambda}}{\mathbf{2}})\mathbf{M}]\mathbf{S} \tag{7}$$

$$S_i = \omega_i\left(\frac{\mathbf{e}_i\cdot\mathbf{F}}{c_s^2} - \frac{(\mathbf{uF}+\mathbf{Fu}):(\mathbf{e}_i\mathbf{e}_i - c_s^2\mathbf{I})}{2c_s^4}\right), \tag{8}$$

where $\boldsymbol{f}(\mathbf{x},t)$ is the distribution function, $\mathbf{e}_i$ is the discrete lattice vectors, $\mathbf{M}$ is the transformation matrix. $\boldsymbol{\Lambda}$ is the diagonal matrix.

The relationship between shear strain rate tensor and non-equilibrium moments can be obtained by using the Chapman–Enskog expansion.

$$\mathbf{m}^{neq} = -\delta_t\boldsymbol{\Lambda}^{-1}\cdot\mathbf{M}\cdot\mathbf{D}_t\cdot\mathbf{M}^{-1}\cdot\mathbf{m}^{eq} + (\boldsymbol{\Lambda}^{-1} - \frac{1}{2}\mathbf{I})\mathbf{MS} \tag{9}$$

where $\mathbf{m}^{neq} = \mathbf{m} - \mathbf{m}^{eq} + \mathbf{MS}/2$ are the non-equilibrium moments, $\mathbf{D}_t = \mathrm{diag}(\partial_t, \partial_t + \mathbf{e_0}\cdot\boldsymbol{\nabla}, \ldots, \partial_t + \mathbf{e_{18}}\cdot\boldsymbol{\nabla})$.

From Eq.(9) and the relationship between the shear strain rate tensor and non-equilibrium moments can be obtained as

$$\begin{cases} m_1^{(neq)} = -\frac{38\rho_0\delta t}{3s_1}\left(\frac{\partial u}{\partial x} + \frac{\partial v}{\partial y} + \frac{\partial w}{\partial z}\right) \\ m_9^{(neq)} = -\frac{2\rho_0\delta t}{3s_v}\left[\frac{2\partial u}{\partial x} - 3\left(\frac{\partial v}{\partial y} + \frac{\partial w}{\partial z}\right)\right] \\ m_{11}^{(neq)} = -\frac{2\rho_0\delta t}{3s_v}\left(\frac{\partial v}{\partial y} - \frac{\partial w}{\partial z}\right) \\ m_{13}^{(neq)} = -\frac{\rho_0\delta t}{3s_v}\left(\frac{\partial u}{\partial y} + \frac{\partial v}{\partial x}\right) \\ m_{14}^{(neq)} = -\frac{\rho_0\delta t}{3s_v}\left(\frac{\partial v}{\partial z} + \frac{\partial w}{\partial y}\right) \\ m_{15}^{(neq)} = -\frac{\rho_0\delta t}{3s_v}\left(\frac{\partial u}{\partial z} + \frac{\partial w}{\partial x}\right) \end{cases} \tag{10}$$

So, the the S_{ij},

$$\begin{cases} S_{12} = -\frac{3}{2\rho_0\delta t}s_v m_{13}^{neq} \\ S_{13} = -\frac{3}{2\rho_0\delta t}s_v m_{15}^{neq} \\ S_{23} = -\frac{3}{2\rho_0\delta t}s_v m_{14}^{neq} \\ S_{11} = -\frac{1}{38\rho_0\delta t}(3s_1 m_1^{neq} + 19 s_v m_9^{neq}) \\ S_{22} = -\frac{1}{76\rho_0\delta t}[2s_1 m_1^{neq} - 19(s_v m_9^{neq} - 3s_v m_{11}^{neq})] \\ S_{33} = -\frac{1}{76\rho_0\delta t}[2s_1 m_1^{neq} - 19(s_v m_9^{neq} + 3s_v m_{11}^{neq})] \end{cases} \tag{11}$$

3 Results and Discussion

3.1 Taylor-Green vortex

Firstly, we choose Taylor-Green vortex as a validation example at Re=1600. Figure 1 and Figure 2 is the instantaneous kinetic energy and the kinetic energy dissipation rate of Taylor-Green vortex. It can be seen that the present results are in good agreement with the reference [19].

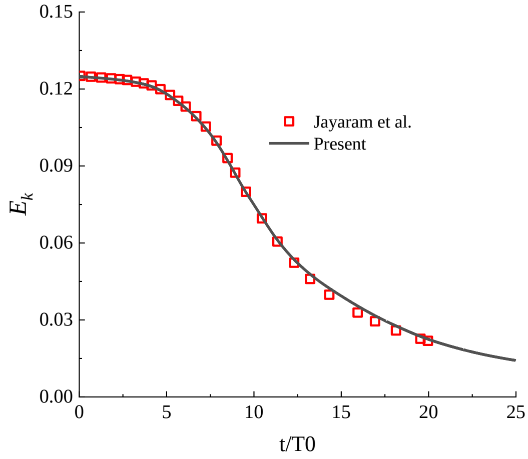

Figure 1 The Taylor-Green vortex instantaneous kinetic energy.

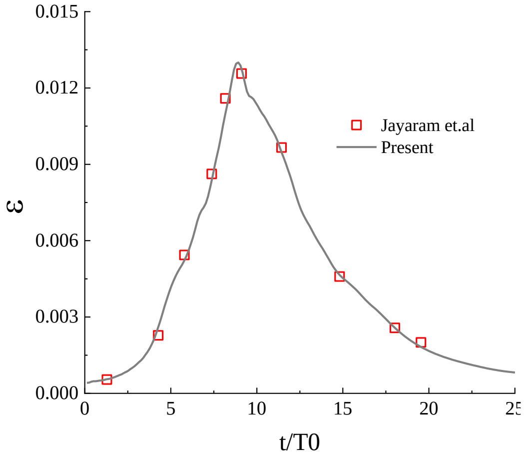

Figure 2 The Taylor-Green vortex instantaneous kinetic energy dissipation rate.

3.2 ABC forcing flow

In addition, we have carried out the verification on the isotropic homogeneous turbulent flow with the body forces in the Arn'old-Beltrami-Childress (ABC) format. Figure 3 presents the results of the turbulent energy spectrum distribution at different Re. The present results of VSS model are basically consistent with those of Smagorinsky model.

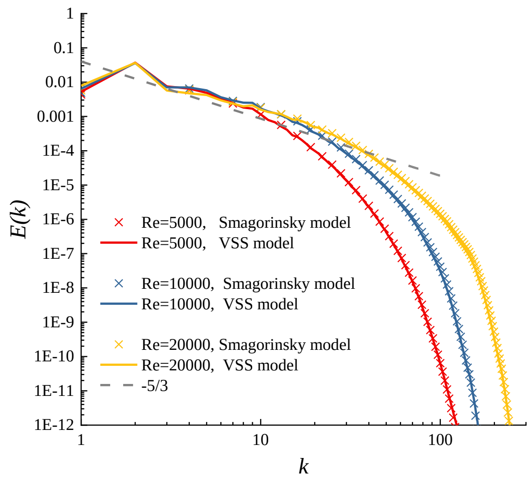

Figure 3 The turbulent energy spectrum distribution at different Re.

3.3 Incompressible turbulent channel flow

The friction Reynolds number is 180. Figure 4 is the mean streamwise velocity profile. The present results of VSS model are in good agreement with the DNS results[20, 21].

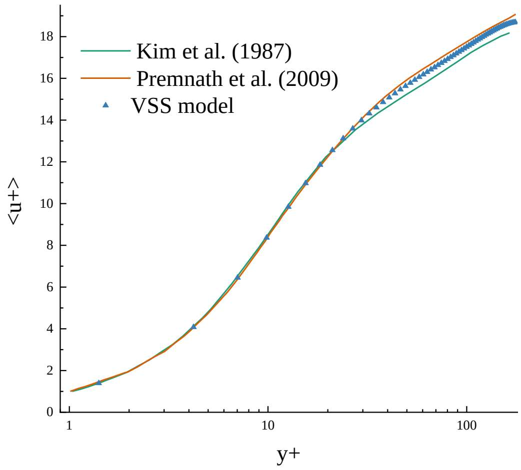

Figure 4 The mean streamwise velocity profile.

4 Conclusion

In this paper, we proposed a new coupling model that combines non-equilibrium moments and the subgrid-scale model was proposed within the framework of the LBM. The coupling model is validated in three incompressible flow cases: Taylor-Green vortex, ABC forcing flow, and the channel flow. The new model is validated by these cases, and the results are good in with the references and the DNS results.

References

[1] ZHANG W, WANG X, KOU J. Prospects of multi-paradigm fusion methods for fluid mechanics research [J]. Advances in Mechanics, 2023, 53: 1-35.
[2] Ren F, Song B, Zhang Y, et al. A GPU-accelerated solver for turbulent flow and scalar transport based on the Lattice Boltzmann method [J]. Computers & Fluids, 2018, 173: 29-36.
[3] Crialesi-Esposito M, Rosti M E, Chibbaro S, et al. Modulation of homogeneous and isotropic turbulence in emulsions [J]. Journal of Fluid Mechanics, 2022, 940.
[4] Bou-Zeid E, Meneveau C, Parlange M. A scale-dependent Lagrangian dynamic model for large eddy simulation of complex turbulent flows [J]. Physics of fluids, 2005, 17(2): 025105.
[5] Argyropoulos C D, Markatos N. Recent advances on the numerical modelling of turbulent flows [J]. Applied Mathematical Modelling, 2015, 39(2): 693-732.
[6] Xia B, Li J. An efficient implementation of nodal discontinuous Galerkin lattice Boltzmann method and validation for direct numerical simulation of turbulent flows [J]. Computers & Mathematics with Applications, 2022, 117: 284-298.
[7] Eshghinejadfard A, Zhao L, Thévenin D. Lattice Boltzmann simulation of resolved oblate spheroids in wall turbulence [J]. Journal of Fluid Mechanics, 2018, 849: 510-540.
[8] Petersen K, Brinkerhoff J. On the lattice Boltzmann method and its application to turbulent, multiphase flows of various fluids including cryogens: A review [J]. Physics of Fluids, 2021, 33(4): 041302.
[9] Teruna C, Avallone F, Casalino D, et al. Numerical investigation of leading edge noise reduction on a rod-airfoil configuration using porous materials and serrations [J]. Journal of Sound and Vibration, 2021, 494: 115880.
[10] Zhang H, Ren F, Hu H B. Transitions of power-law fluids in two-dimensional lid-driven cavity flow using lattice Boltzmann method [J]. Acta Physica Sinica, 2021, 70(18).
[11] Yu H, Luo L-S, Girimaji S S. LES of turbulent square jet flow using an MRT lattice Boltzmann model [J]. Computers & fluids, 2006, 35(8-9): 957-965.
[12] Xia Z, Shi Y, Chen Y, et al. Comparisons of different implementations of turbulence modelling in lattice Boltzmann method [J]. Journal of Turbulence, 2015, 16(1): 67-80.

[13] Smagorinsky J. General circulation experiments with the primitive equations: I. The basic experiment [J]. Monthly weather review, 1963, 91(3): 99-164.

[14] Vreman A. An eddy-viscosity subgrid-scale model for turbulent shear flow: Algebraic theory and applications [J]. Physics of fluids, 2004, 16(10): 3670-3681.

[15] Germano M, Piomelli U, Moin P, et al. A dynamic subgrid-scale eddy viscosity model [J]. Physics of Fluids A: Fluid Dynamics, 1991, 3(7): 1760-1765.

[16] Nicoud F, Ducros F. Subgrid-scale stress modelling based on the square of the velocity gradient tensor [J]. Flow Turbulence and Combustion, 1999, 62(3): 183-200.

[17] Nicoud F, Toda H B, Cabrit O, et al. Using singular values to build a subgrid-scale model for large eddy simulations [J]. Physics of fluids, 2011, 23(8): 085106.

[18] Ryu S, Iaccarino G. A subgrid-scale eddy-viscosity model based on the volumetric strain-stretching [J]. Physics of Fluids, 2014, 26(6): 065107.

[19] Jayaram R, Jie Y, Zhao L, et al. Clustering of inertial spheres in evolving Taylor–Green vortex flow [J]. Physics of Fluids, 2020, 32(4): 043306.

[20] Premnath K N, Pattison M J, Banerjee S. Generalized lattice Boltzmann equation with forcing term for computation of wall-bounded turbulent flows [J]. Physical Review E, 2009, 79(2): 026703.

[21] Kim J, Moin P, Moser R. Turbulence statistics in fully developed channel flow at low Reynolds number [J]. Journal of fluid mechanics, 1987, 177: 133-166.